ISSN 1330-3651
UDC/UDK 621.791.05:620.172.24]:519.6

NUMERICAL ANALYSIS OF CONSTRAINT EFFECT ON DUCTILE TEARING IN STRENGTH MISMATCHED WELDED CCT SPECIMENS USING MICROMECHANICAL APPROACH

Bashir Younise, Marko Rakin, Bojan Medjo, Nenad Gubeljak, Dražan Kozak, Aleksandar Sedmak

Original scientific paper

In this paper, constraint effect on ductile fracture initiation and propagation has been studied. Three-dimensional finite element analyses of mismatched welded joints made of high strength steel, have been performed for centre-cracked tensile (CCT) specimens. Different weld widths and material mismatching ratios have been considered. Ductile fracture parameter, crack tip opening displacement at crack growth initiation ($CTOD_i$), has been obtained for centre-cracked tensile (CCT) specimens using local approach to fracture and compared with experimental results of single edge bend specimens. Micromechanical complete Gurson model has been applied to investigate fracture behaviour of cracked welded joints. Crack tip constraint has been analysed through stress triaxiality in order to study transferability of fracture parameters from one geometry to another.

Keywords: *constraint effect, ductile fracture, finite element analysis, material mismatching, stress triaxiality, transferability*

Numerička analiza efekta ograničenja duktilnog cijepanja na zavarenim CCT uzorcima nejednake čvrstoće uz primjenu mikromehaničkog pristupa

Izvorni znanstveni članak

U ovom radu su istraženi efekti ograničenja na inicijaciju i propagaciju žilavog loma. Trodimenzionalna analiza konačnim elementima zavarenih spojeva nejednake čvrstoće, izrađenih od visokočvrstog čelika, pokazana je na primjeru CCT uzoraka sa središnjom pukotinom opterećenih na rastezanje. Razmatrane su različite širine zavara i omjeri nejednakosti čvrstoće. Parametar žilavog loma, pomak otvaranja vrška pukotine pri inicijaciji rasta pukotine ($CTOD_i$), dobiven je za CCT uzorak sa zarezom u sredini opterećenim na vlak koristeći lokalni pristup lomu, uz usporedbu s eksperimentalnim rezultatima određenim na uzorku na savijanje zarezanim s jedne strane. Mikromehanički cjeloviti Gursonov model primijenjen je kako bi se istražilo lomno ponašanje zavarenih spojeva s pukotinom. Ograničenja tečenja oko vrška pukotine analizirani su kroz troosnost naprezanja, kako bi se istražila prenosivost parametara loma s jedne geometrije na drugu.

Ključne riječi: *analiza metodom konačnih elemenata, efekt ograničenja, nejednakost materijala u spoju, prenosivost, troosnost naprezanja, žilavi lom*

1 Introduction
Uvod

High strength steels exhibit plastic straining and large scale deformation during tearing. The fracture behaviour of such steels cannot be accurately predicted by conventional fracture mechanics parameters such as *J*-integral or crack tip opening displacement (CTOD). Additionally, they cannot adequately characterize the crack tip stress field. Therefore, more accurate methods are of particular interest for failure assessment in high strength steels.

Local damage models have been extensively used in the last decade to investigate fracture behaviour in ductile materials. They can simulate the process of void nucleation, growth and coalescence in the material. These models link material fracture behaviour to the parameters that describe the evolution of micro-voids rather than the conventional global fracture parameters which cannot be directly transferred from one geometry to another. Local damage parameters are dependent only on material, and not on geometry.

Ductile fracture process is often modelled by means of the Gurson model [1], which describes the progressive degradation of material load carrying capacity. This model has been later modified by Tvergaard and Needleman [2, 3], the resultant model is not intrinsically able to predict coalescence, and is only capable of simulating nucleation and growth of micro-voids. This deficiency is solved by introducing an empirical void coalescence criterion: coalescence occurs when a critical void volume fraction, f_c, is reached. The value of f_c is introduced in the model as a constant value which depends on material. Several studies have shown different values of f_c can be obtained from the same tension tests [4]. Therefore, a complete Gurson model (CGM) has been introduced by Zhang et al. [5], who combined the Gurson-Tvergaard-Needlman (GTN) model and the coalescence criterion proposed by Thomason [4]. CGM has considered critical void volume fraction, f_c, is not a material constant but it depends on the stress state and the geometry. The model has been implemented in FORTRAN and it has been introduced in the ABAQUS finite element code by means of the UMAT user subroutine developed by Zhang, based on [5]. The complete Gurson model has been shown to give accurate predictions for different levels of stress triaxiality, for strain non-hardening and strain hardening materials.

The aim of this work was to simulate ductile fracture initiation and propagation in high strength steel weldments using the complete Gurson model. Three-dimensional finite element models for welded CCT plates with different strength mismatching and weld widths were developed to study fracture behaviour of welded high strength steel. Ductile fracture initiation for different strength mismatching and weld widths has been predicted. The effect of crack tip constraint on ductile fracture initiation and propagation has been studied too. Fracture resistance curves have been obtained to characterise the fracture behaviour.

2 Modelling of ductile tearing
Modeliranje odcjepnog žilavog loma

Micromechanical models have been developed for modelling the behaviour of ductile materials. Among these models, the model proposed by Gurson is considered, as very widely used one for ductile porous materials. The yield function of Gurson [1], modified by Tvergaard [6, 7] and Tvergaard and Needleman [2, 8], is used to describe the

evolution of void growth and subsequent macroscopic softening. The modified yield function is defined by formula:

$$\phi(q,\sigma_{\mathrm{m}},\sigma,f) = \\ =\left(\frac{q}{\bar{\sigma}}\right)^2 + 2q_1 f^* \cosh\left(\frac{3q_2\sigma_{\mathrm{m}}}{2\bar{\sigma}}\right)^2 - \left(1+\left(q_1 f^*\right)^2\right) = 0 \quad (1)$$

where σ_{m} is the mean stress, $\bar{\sigma}$ is the flow stress of the matrix material, f* is the modified void volume fraction, and q is the von Mises effective stress:

$$q = \sqrt{\frac{3}{2} S_{ij} S_{ij}}, \quad (2)$$

where S_{ij} stand for the deviatoric components of the stress tensor. The constants q_1 and q_2 are fitting parameters introduced by Tvergaard [6] to improve the ductile fracture prediction of Gurson model. These constants are q_1=1,5 and q_2=1, which are usual values for metallic materials. The modified void volume fraction, f*, is the damage function [2] given by

$$f^* = \begin{cases} f & \text{for} \quad f \le f_{\mathrm{c}} \\ f_{\mathrm{c}} + \dfrac{f_{\mathrm{u}}^* - f_{\mathrm{c}}}{f_{\mathrm{F}} - f_{\mathrm{c}}}\left(f - f_{\mathrm{c}}\right) & \text{for} \quad f > f_{\mathrm{c}} \end{cases} \quad (3)$$

where f_{c} is the critical void volume fraction at the moment the void coalescence occurs, $f_{\mathrm{u}}^* = 1/q_1$ is the ultimate void volume fraction, and f_{F} is the void volume fraction at final failure.

The increase of the void volume fraction, f, during increment of deformation is partly due to the growth of existing voids and partly due to the nucleation of new voids. Thus the evolution law for the void volume fraction is given in the form:

$$\dot{f} = \dot{f}_{\mathrm{nucleation}} + \dot{f}_{\mathrm{growth}}. \quad (4)$$

Nucleation is considered to depend exclusively on the effective strain in the material and can be estimated by the following equation:

$$\dot{f}_{\mathrm{nucleation}} = A\dot{\varepsilon}_{\mathrm{eq}}^{\mathrm{p}}, \quad (5)$$

where $\dot{\varepsilon}_{\mathrm{eq}}^{\mathrm{p}}$ is the equivalent plastic strain rate; parameter A is scalar constant concerning the damage acceleration. It is estimated by the following expression, proposed by Chu and Needleman [9]:

$$A = \frac{f_{\mathrm{N}}}{S_{\mathrm{N}}\sqrt{2\pi}} \exp\left[-\frac{1}{2}\left(\frac{\bar{\varepsilon}_{\mathrm{eq}} - \varepsilon_{\mathrm{N}}}{S_{\mathrm{N}}}\right)^2\right], \quad (6)$$

f_{N} is the void volume fraction of nucleating particles, ε_{N} is the mean strain for void nucleation and S_{N} is the corresponding standard deviation.

The void volume fraction due to growth can be estimated by:

$$\dot{f}_{\mathrm{growth}} = (1-f)\dot{\varepsilon}_{ii}^{\mathrm{p}}, \quad (7)$$

where $\dot{\varepsilon}_{ii}^{\mathrm{p}}$ is plastic part of the strain rate tensor.

The critical void volume fraction, f_c, is not considered as a material constant in complete Gurson model. It is determined by Thomason's plastic limit-load criterion, which predicts the onset of coalescence when the following condition is satisfied [4]:

$$\frac{\sigma_1}{\bar{\sigma}} \ge \left(\alpha\left(\frac{1}{r}-1\right)^2 + \frac{\beta}{\sqrt{r}}\right)\left(1-\pi r^2\right) \quad (8)$$

where α = 0,1 and β =1,2 are two constants fitted by Thomason, σ_1 is the maximum principal stress and r is the void space ratio given by the formula:

$$r = \sqrt[3]{\frac{3f}{4\pi}\mathrm{e}^{\varepsilon_1+\varepsilon_2+\varepsilon_3}}\left(\frac{\sqrt{\mathrm{e}^{\varepsilon_2+\varepsilon_3}}}{2}\right)^{-1} \quad (9)$$

where ε_1, ε_2 and ε_3 are the principal strains.

The complete Gurson model, which is used in this work, was implemented into the finite element code ABAQUS through the material user subroutine UMAT, which has been developed by Zhang, based on [5].

3 Material characterization
Karakterizacija materijala

The material studied in this investigation was high strength steel, NIOMOL 490K, which is often used for pressure vessels. Under- and overmatched welded CCT plates with different joint widths have been used to study the effect of strength mismatching and crack tip constraint on fracture initiation and propagation. The mismatch factor of materials is defined by the expression:

$$M = \frac{R_{\mathrm{p\,0,2WM}}}{R_{\mathrm{p\,0,2BM}}} \quad (10)$$

where $R_{\mathrm{p0,2WM}}$ and $R_{\mathrm{p0,2BM}}$ are yield strengths of the weld and base metals, respectively. Mechanical properties are given in Tab. 1 for used materials. The Poisson's ratio was assumed to be ν = 0,3.

Table 1 *Mechanical properties of the base and weld metals at room temperature*
Tablica 1. *Mehanička svojstva osnovnog materijala i metala zavara na sobnoj temperaturi*

Material	Young's modules E / GPa	Yield stress $R_{\mathrm{p0,2}}$ / MPa	Tensile strength R_{m} / MPa	Mismatching factor M
Over-matching	183,8	648	744	1,19
Base metal	202,9	545	648	-
Under-matching	206,7	469	590	0,86

The initial void volume fraction, f_0 = 0,002, and the void volume fraction of nucleating particles, f_{N} = 0, have been previously used for the same materials in [10].

4
Numerical procedure
Numerička procedura

Mechanical properties of investigated materials were obtained at room temperature. True stress-true strain data given in Fig. 1 were used in numerical modelling.

Geometry of welded CCT specimen given in Fig. 2 with a ratio of crack length to width; $a_0/W = 0{,}35$, width; $2W = 40$ mm, and thickness; $B = 10$ mm have been modelled.

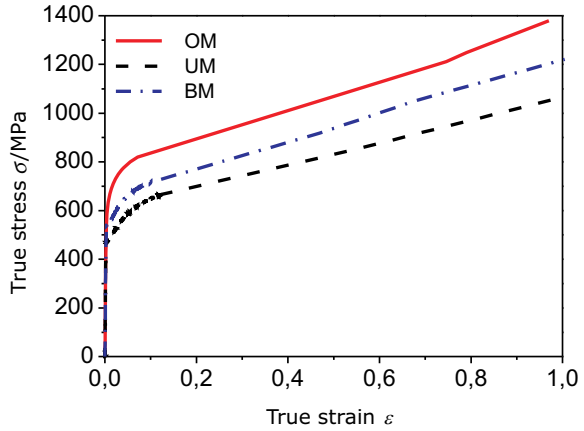

Figure 1 *True stress-true strain curves of materials*
Slika 1. *Stvarni dijagram tečenja materijala*

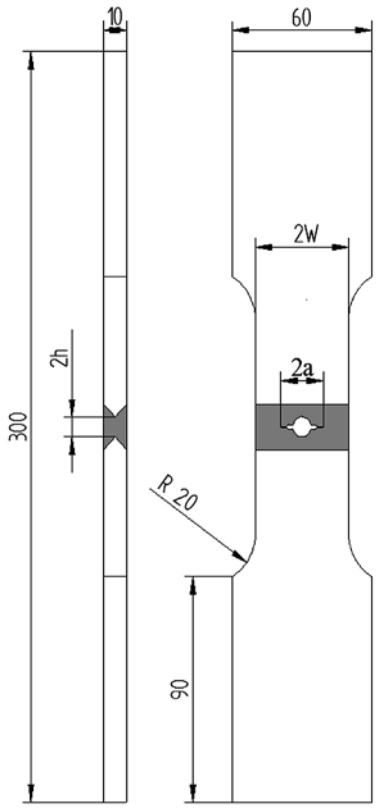

Figure 2 *Geometry of CCT specimen*
Slika 2. *Geometrija CCT uzorka*

Welded specimens are considered as bimaterial joints, since the crack is located in the weld metal, along the axis of symmetry of the weld. Two different widths of the weld metal for both overmatched (OM) and undermatched (UM) welded joints were considered: $2h = 6$ and 18 mm.

Many researchers [11-13] have modelled the entire specimen or structure using damage constitutive relations to study the ductile fracture of metals. However, from metallurgical observations of ductile tearing [14], it has been found that many metals have a macroscopically planar fracture process zone. That is, damage is restricted to a region around the prospective crack plane. Thus, modelling the whole specimen or structure using a damage constitutive model is unnecessary and inefficient in terms of computational economy. Several researchers [15, 16] have introduced a single layer of elements with a damage constitutive model, namely computational cells, in front of the prospective crack plane to simulate the ductile tearing. This procedure has been adopted herein.

Finite element code ABAQUS [17] with material user subroutine UMAT [5] has been used to model centre cracked specimen. Three-dimensional finite element meshes were generated in order to estimate ductile fracture initiation values and crack propagation. Fig. 3 shows finite element mesh employed to model CCT specimen. Due to symmetry about X, Y, and Z planes, only one eighth of the specimen was modelled. Three-dimensional eight-noded linear brick (C3D8) elements were used in the model.

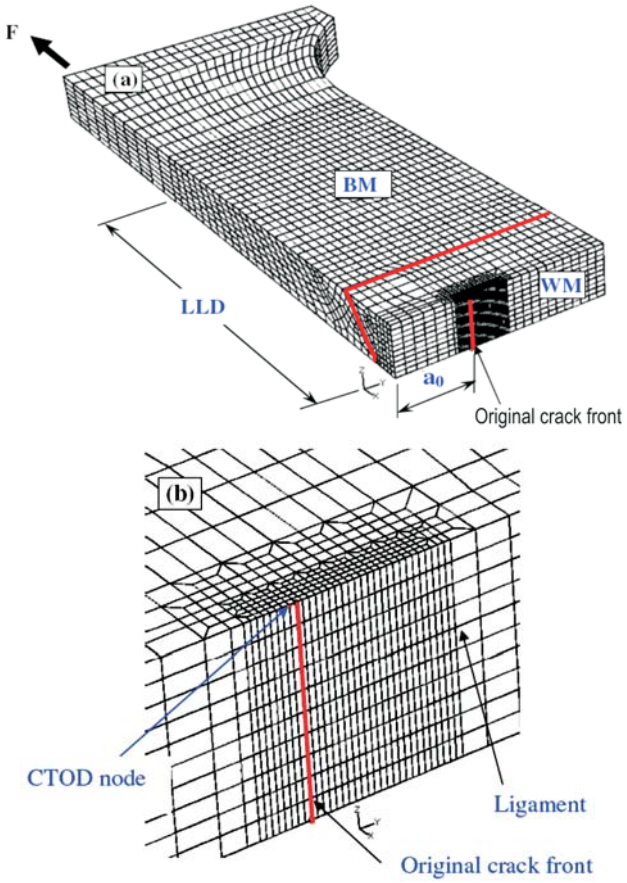

Figure 3 *Three-dimensional finite element model for CCT specimen. (a) 3D finite element mesh for one eighth of specimen. (b) Detailed mesh for the region near the crack front*
Slika 3. *Trodimenzionalni model konačnih elemenata za CCT uzorak. (a) 3D mreža konačnih elemenata 1/8 uzorka. (b) Detaljna mreža područja u blizini fronte pukotine*

In the model of the tearing zone, ahead the crack front, four layers of elements with a highly refined mesh stretch out across the ligament ahead of the crack tip because of expected damage and crack propagation in this region. Coarse meshes are applied beyond this region where no significant material degradation is anticipated. The mesh size, l_0, was adopted previously for used material [10]. A

fixed mesh size $l_0 = 0{,}15$ mm of elements was chosen in X-Y plane near crack tip, but in Z-direction is about 3 l_0 because damage propagation in that direction is not pronounced.

Symmetry boundary conditions were applied to the boundary surfaces at X = 0, Y = 0, and Z = 0. The applied load was simulated by prescribed displacement along X-axis at the end of the specimen side, as shown in Fig. 3(a).

4.1
Modelling of ductile fracture initiation
Modeliranje inicijacije žilavog loma

Ductile fracture initiation, described here by crack tip opening displacement at crack growth initiation $CTOD_i$, is modelled for different joint widths and strength mismatching based on critical void volume fraction criterion, f_c, which represents the end of stable void growth and the start of void coalescence in the material. Most researchers assume it to be a material constant. However, experimental studies [18] indicated a variation of the critical void volume fraction as a function of stress triaxiality. Thomason [4] indicated that void coalescence results essentially from the attainment of a plastic limit-load, inducing failure of the intervoid matrix. Therefore, f_c is not a material constant according to the complete Gurson model, which is developed on the basis of plastic limit-load.

The condition for the onset of crack growth, as determined by the J-integral at initiation J_i, is most adequately defined by the micro-mechanical criterion [10]:

$$f \geq f_c . \tag{11}$$

When the condition given by Eq. (11) is satisfied, the onset of the crack growth occurs. Ductile fracture initiation is described here by the crack tip opening displacement at crack growth initiation ($CTOD_i$). This value was estimated by complete Gurson model when the critical void volume fraction, f_c, is reached.

Ductile crack growth initiation is estimated numerically when void volume fraction, f, at gauss integration points of elements in front of the crack line reaches critical value, f_c, and equation (11) is satisfied.

4.2
Modelling of ductile fracture propagation
Modeliranje propagacije žilavog loma

Ductile fracture propagation in finite element methods can be simulated by four techniques; element splitting, element deleting, node releasing, and stiffness decreasing. The last method has been used to simulate the crack growth in this work.

The CTOD value is extracted from a fixed node in front of the initial crack line, which can be seen in Fig. 3(b). The element is assumed to fail (completely lost load carrying capacity) when the void volume fraction at final failure is reached. Then, crack growth, Δa, can be simulated by tracing the path of completely damaged elements, which appears completely in red colour in this work. In other words, the crack growth can be estimated by multiplying the original length, l_0, with the number of damaged elements.

5
Results and discussion
Rezultati i rasprava

5.1
Crack growth initiation
Inicijacija rasta pukotine

The values of the crack tip opening displacement at crack growth initiation, $CTOD_i$, have been numerically estimated at the middle of the specimen thickness in front of the crack line, where the highest value of void volume fraction are obtained. Fig. 4 shows the distribution of void volume fraction, f, along crack front at the moment of the crack growth initiation for overmatched welded joint with weld width, $2h = 6$ mm. The values of $CTOD_i$ have been numerically estimated for CCT specimens with different strength mismatching and weld widths and given in Tabs. 2 and 3 in comparison with experimental results for SE(B) specimen [10]. The numerical results in Tab. 2 have been obtained using the CGM. However, they have been numerically obtained using GTN (Gurson-Tvergaard-Needlman) model in [10]. The geometry of SE(B) specimen was as follows: the ratio of crack length to width: $a_0/W = 0{,}32$, thickness: $B = 25$ mm, and specimen width: $W = B$, [10].

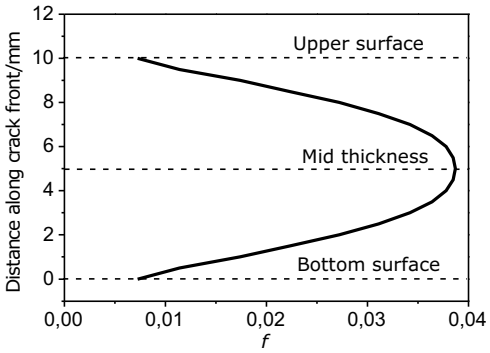

Figure 4 *Void volume fraction, f, distribution along the crack front at the moment of crack growth initiation for overmatched welded joint with weld width 6 mm*
Slika 4. *Volumenski udjel praznina, f, raspodjela uzduž fronte pukotine u trenutku inicijacije rasta pukotine za zavareni spoj više granice tečenja od osnovnog materijala uz širinu zavara 6 mm*

It can be observed in Tabs. 2 and 3 that $CTOD_i$ values for welded CCT specimens are higher than those for the welded single edge bend specimens due to the higher level of crack tip constraint in front of crack line for the latter ones.

Table 2 *Experimental and numerical values of $CTOD_i$ for SE(B) specimens in OM and UM welded joints* [10]
Tablica 2. *Eksperimentalne i numeričke vrijednosti $CTOD_i$ za SE(B) uzorak u OM i UM zavarenim spojevima* [10]

Specimen type		$CTOD_i$ / mm			
		$2h = 6$ mm		$2h = 18$ mm	
		Exper.	Num.	Exper.	Num.
SE(B)	OM	0,084	0,157	0,065	0,129
	UM	0,120	0,119	0,132	0,130

It can be observed in Tabs. 2 and 3 that $CTOD_i$ values for welded CCT specimens are higher than those for the welded single edge bend specimens due to the higher level of crack tip constraint in front of crack line for the latter

Table 3 *Numerical values of CTOD$_i$ for CCT specimens in OM and UM welded joints*
Tablica 3. *Numeričke vrijednosti CTOD$_i$ za CCT uzorke u OM i UM zavarenim spojevima*

Specimen type		CTOD$_i$ / mm	
		$2h$ = 6 mm	$2h$ = 18 mm
		Num.	Num.
CCT	OM	0,505	0,435
	UM	0,284	0,365

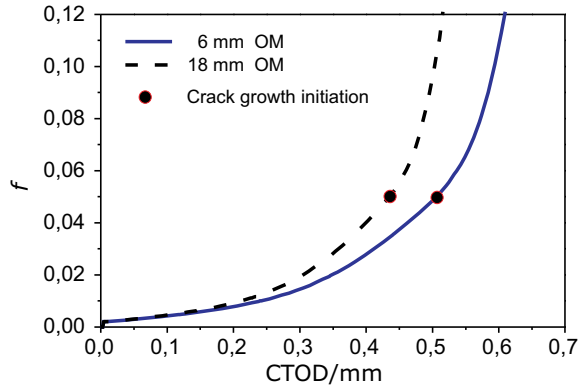

Figure 5 *Void volume fraction, f , vs. crack tip opening displacement, CTOD, for OM welded CCT specimens*
Slika 5. *Ovisnost volumenskog udjela praznina , f i pomaka vrška otvaranja pukotine, CTOD, za OM zavarenih CCT uzoraka*

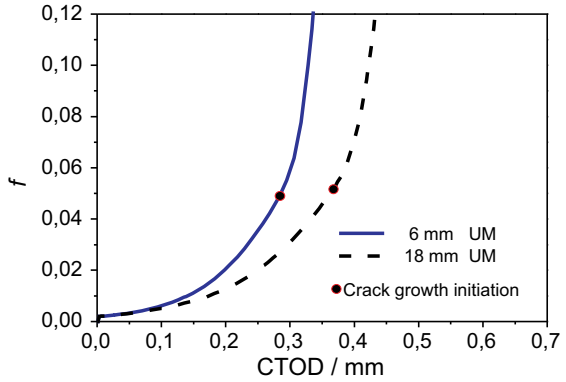

Figure 6 *Void volume fraction, f vs. crack tip opening displacement, CTOD, for UM welded CCT specimens*
Slika 6. *Ovisnost volumenskog udjela praznina, f i pomaka vrška otvaranja pukotine, CTOD, za UM zavarenih CCT uzoraka*

ones.

Figs. 5 and 6, show the rate of void volume fraction, *f*, with respect to CTOD in overmatched welded joint with larger width is higher than the one in overmatched welded joint with smaller width, while the opposite phenomenon occurs in undermatched welded joints. Therefore, overmatched welded joints with smaller weld width have higher crack growth initiation resistance than those with wider width, and vice versa in case of undermatched welded joints (see Tabs. 2 and 3). These results are in agreement with experimental results given in [19].

5.2
Ductile fracture propagation
Širenje žilavog loma

Crack growth has been simulated by tracing the path of damaged elements which can be seen in red colour in the cross section of the model (Fig. 7). When the elements in front of the crack line become completely red, which indicates the void volume fraction, *f*, reaches the failure value, f_F, the crack growth is measured according to standards such as; ASTM E1820 [20], as can be seen in Fig. 7 and corresponding CTOD value to that crack growth is measured at CTOD node. The crack growth extension, Δa, is measured up to the current crack front at nine equally spaced points. The first two measurements at the outer points are averaged and then this value is averaged with the seven inner points.

The fracture resistance curves for different strength mismatching and weld widths have been estimated by the explained technique. Fig. 8 shows CTOD-*R* resistance curves for different strength mismatched welded joints with different weld widths. It can be seen in Fig. 8 that the highest fracture resistance has been obtained for overmatched welded CCT specimen with smaller weld width while the lowest fracture resistance has been obtained for undermatched welded CCT specimen with smaller weld width. These effects of strength mismatching and weld width on crack growth resistance are in agreement with experimental results obtained in [21] on welded standard specimens (single edge bend specimen) with different strength mismatching and weld widths.

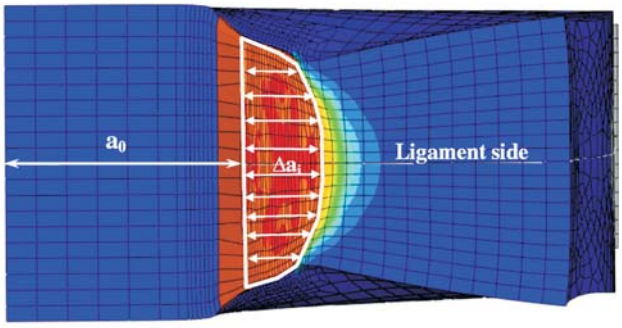

Figure 7 *Distribution of void volume fraction, f, in the cross section of CCT specimen with crack growth measurement*
Slika 7. *Raspodjela volumenskog udjela praznina, f u poprečnom presjeku CCT uzorka s mjerenjem rasta pukotine*

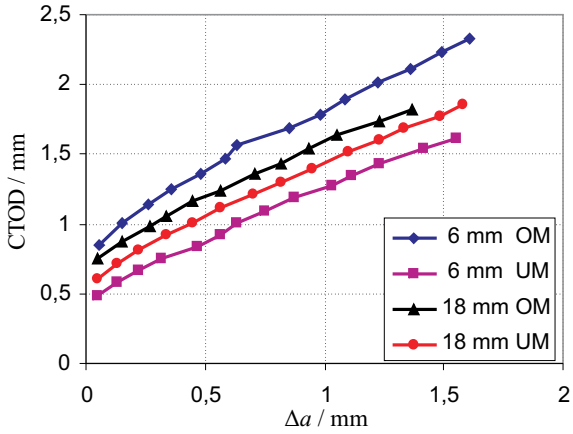

Figure 8 *CTOD-R resistance curves for different strength mismatching and weld widths*
Slika 8. *CTOD-R krivulje otpornosti za različite nejednakosti čvrstoće materijala u spoju i širine zavara*

5.3
Constraint effects on ductile fracture
Učinci ograničenja na žilavi lom

The choice of specimens for structural integrity assessment in conventional fracture mechanics depends on constraint level - if the constraint level of the specimen matches the constraint level of the component, the results of

specimen seem to be transferred to that of component within certain circumstances. Thus, micromechanical models do not depend on parameters which cannot be transferred directly from one geometry to another, but it depends on material parameters which are considered constant and can be transferred.

Several studies [22-24] have shown that material strength mismatching significantly affects both the stress fields and the crack growth curves of tension and bend specimens [25-27]. That is, constraint is not only a function in geometry, but also of material mismatching. Thus, in addition to any geometrical constraint, constraint due to material mismatching should be taken into account [28-40].

To understand fracture behaviour of mismatched welded structures, constraint level has been analysed using stress triaxiality, which is defined as the ratio of mean stress to the equivalent von Mises stress. Constraint effect has been studied for different strength mismatching and weld widths in front of the initial crack front along the ligament in the middle of the specimen thickness. It can be observed in Fig. 9 that the effect of strength mismatching changes on stress triaxiality is higher than the effect of weld width changes. While the effect of weld width changes in overmatched welded joints on stress triaxiality is higher than the effect of weld width changes in undermatched welded joints.

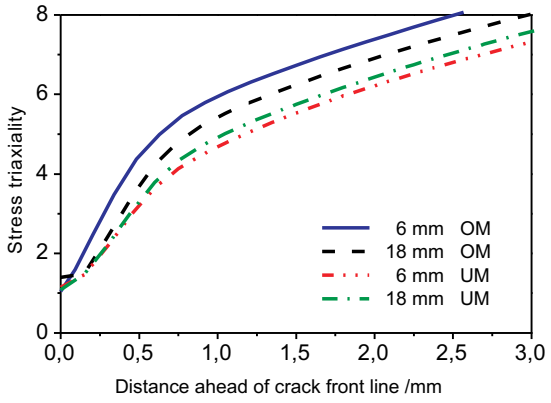

Figure 9 *Stress triaxiality ahead of the initial crack front for different strength mismatching and weld widths at the moment of crack growth initiation*

Slika 9. *Troosnost naprezanja uzduž inicijalne fronte pukotine za različite nejednakosti čvrstoće i širine zavara u trenutku inicijacije rasta pukotine*

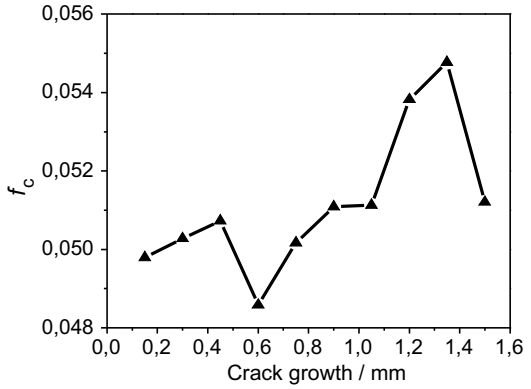

Figure 10 *Variation of critical void volume fraction, f_c, at the crack tip along crack growth path for weld width of 6 mm and overmatched CCT specimen*

Slika 10. *Promjena kritičnog volumenskog udjela praznina, f_c, na vršku pukotine uzduž putanje rasta pukotine za širinu zavara 6 mm i CCT uzorak sa zavarom više čvrstoće od osnovnog materijala*

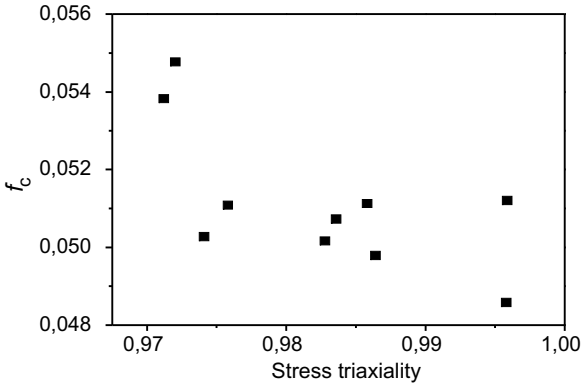

Figure 11 *Critical void volume fraction, f_c, vs. stress triaxiality at the crack tip along crack growth path for weld width of 6 mm and overmatched CCT specimen*

Slika 11. *Kritični volumenski udjel praznina, f_c, u odnosu na troosnost naprezanja na vršku pukotine uzduž putanje rasta pukotine za zavar širine 6 mm i CCT uzorak sa zavarom više čvrstoće od osnovnog metala*

As mentioned previously, the failure criterion of the complete Gurson model (critical void volume fraction, f_c) is not a material constant [5]. Since it is determined on the basis of plastic limit load criterion [4], it depends on stress and strain state in the structure, i.e. competition between the homogeneous and localised deformation modes during ductile fracture process. This causes the critical void volume fraction to depend on constraints caused by change of structure geometry, crack geometry and material properties around the crack tip. Since the stress and strain fields depend on mentioned constraints in all materials, the fact that the CGM failure criterion is not a material parameter is valid irrespective of material type (e.g. for both ferrous and nonferrous metallic materials).

Fig. 10 shows the variations of f_c at crack front along the path of the crack growth. f_c was obtained from the element that failed first. The results show that the value of f_c varied significantly along the crack growth path. Thus, the value f_c may not be transferred from one geometry to another as a constant value due to different stress triaxiality among them. The effect of stress triaxiality on f_c along the path of the crack growth can also be seen in Fig. 11.

6 Conclusion
Zaključak

The effect of constraint on fracture initiation and propagation has been studied for strength mismatched welded joints with different weld widths. Micromechanical complete Gurson model has been applied. Different strength mismatching and weld widths have been considered for centre cracked specimens to analyze the effect of constraint on fracture behaviour using stress triaxiality. The following conclusions are drawn from this analysis:

- Ductile fracture initiation and propagation in CCT specimens have been modelled by complete Gurson model. The results have shown that the CCT specimen is less conservative specimen than SE(B) one.
- Once damage material parameters have been determined on specimens, they can be transferred from specimens to components to predict fracture behaviour of different geometries.
- In modelling of fracture resistance behaviour, the crack growth can be simulated by continuous damage process

without using conventional techniques such as nodal release, which likely poses numerical instability.

- The variation of strength mismatching has higher effect on fracture behaviour in comparison with the variation of weld width.
- Stress triaxiality in front of the crack front has remarkable effect on failure criterion, f_c, which is a natural outcome of the material response.

Acknowledgment
Zahvala

Marko Rakin, Bojan Medjo and Aleksandar Sedmak acknowledge the support from the Serbian Ministry of Science under the project OI 174004. This work is also supported through Croatian-Serbian bilateral project. Authors would also like to thank Z. L. Zhang for the CGM user subroutine.

7
References
Literatura

[1] Gurson, Al. Continuum theory of ductile rupture by void nucleation and growth, Part I. yield criteria and flow rules for porous ductile media. // J Engng Mater Tech. 99, (1977), pp. 2-15.
[2] Tvergaard, V.; Needleman, A. Analysis of cup-cone fracture in a round tensile bar. // Acta metal. 32, (1984), pp. 57-169.
[3] Needleman, A.; Tvergaard, V. An analysis of ductile rapture in notched bars. // J Mech Phys Solids. 32, (1984), pp. 461-90.
[4] Thomason, P. F. Ductile fracture of metals. Oxford: Pergamon Press; 1990.
[5] Zhang, Z. L.; Thaulow, C.; Odegard, J. A complete Gurson model approach for ductile fracture. // Engng Fract Mech. 67, (2000), pp. 155-68.
[6] Tvergaard, V. Influence of voids on shear bands instabilities under plane strain conditions. // Int J Fract. 17, (1981), pp. 389-407.
[7] Tvergaard, V. On localization in ductile materials containing spherical voids. // Int J Fract, 18, (1982), pp.157-69.
[8] Tvergaard, V. Material failure by void growth to coalescence. // Adv Appl Mech. 27, (1990), pp. 83-151.
[9] Chu, C.; Needlman, A. Void nucleation effects in biaxiality stretched sheets. // ASME, Journal of Engineering Materials and Technology. 102, (1980), pp. 249-256.
[10] Rakin, M.; Gubeljak, N.; Dobrojević, M.; Sedmak, A. Modelling of ductile fracture initiation in strength mismatched welded joint. // Eng. Fract. Mech. 75, (2008), pp. 3499-3510.
[11] Pardeon, T.; Doghri, I.; Delannay, F. Experimental and numerical comparison of void growth models and void coalescence criteria for the prediction of ductile fracture in copper bars. // Acta Mater. 46, (1998), pp. 541-552.
[12] Baaser, H.; Gross, D. Crack analysis in ductile cylindrical shells using Gurson's model. // International Journal of solids and structures. 37, (2000), pp. 7093-7104.
[13] Besson, J.; Steglich, D.; Brocks, W. Modeling of crack growth in round bars and plane strain specimens. // International Journal of solids and structures 38, (2001), pp. 8259-84.
[14] Van Stone, R.; Cox, T.; Low, J.; Psioda, J. Microstructural aspects of fracture by dimpled rupture. // International Metals Reviews. 30, (1985), pp. 157-179.
[15] Ruggieri, C.; Panontin, T. L.; Dodds, R. H. Numerical modeling of ductile crack growth in 3-D using computational cell elements. // International Journal of Fracture. 82, (1996), pp. 76-95.
[16] Gao, X.; Faleskog, J.; Shih, F. Cell model for nonlinear fracture analysis-II. Fracture process calibration and verification. // International Journal of Fracture. 89, (1998), pp. 375-389.
[17] ABAQUS, version 6.7. Hibbit, Karlsson, and Sorensen (HKS) Inc. Pawtucket, 2007.
[18] Shi Y. W.; Barnby J. T.; Nadkarni A. S. Void growth at ductile crack initiation of a structural steel. // Engineering Fracture Mechanics. 39, (1991), pp. 37-44.
[19] Gubeljak, N.; Scheider, I.; Kocak, M.; Predan, J. Constraint effect on fracture behaviour or strength mismatched weld joint. // in: 14 European Conference on Fracture. EMAS publishing, (2002), pp. 647-655.
[20] ASTM E1820-99a: Standard Test Method for measurement of fracture toughness, ASTM, USA, 1999.
[21] Penuelas, I.; Betegon, C.; Rodriguez, C. A ductile failure model applied to the determination of the fracture toughness of welded joints. Numerical simulation and experimental validation. // Eng. Fract. Mech. 73, (2006), pp. 2756-2773.
[22] Hao, S.; Schwalbe, K. H.; Cornec, A. The effect of yield strength mismatch on the fracture analysis of welded joints: slip-line field solutions for pure bending. // I. J solids struct. 37, (2000), pp. 5385-411.
[23] Joch, J.; Ainsworth, R. A., Hyde, T. H. Limit load and *J*-estimates for idealized problems of deeply cracked welded joints in plane-strain bending. // Fatigue Fract Engng Mater sruct. 16, (1993), pp. 1061-79.
[24] Burstow, M. C.; Ainsworth, R. A. Comparison of analytical, numerical and experimental solutions to problems of deeply cracked welded joints in bending. // Fatigue Fract Engng Mater sruct. 18, (1995), pp. 221-34.
[25] Kirk, M. T.; Dodds, R. H. The influence of weld strength mismatch on crack-tip constraint in single edge notch bend specimens. // Int J Fract. 18, (1993), pp. 279-316.
[26] Burstow, M. C.; Howard, I. C.; Ainsworth, R. A. The influence of constraint on crack tip stress fields in strength mismatched welded joints. // J Mech Phys solids. 46, (1998), pp. 845-72.
[27] Burstow, M. C.; Howard, I. C. Constraint effects on crack growth resistance curves of strength mismatched welded specimens. In: Schwalbe KH, Koçak M, editors. Mismatching of interfaces and welds. // Geesthacht, FRG: GKSS Research Center Publications. (1997), pp. 357-69.
[28] Kim, Y. J.; Schwalbe, K. H. Numerical analysis of strength-mismatch effect on local stresses for ideally plastic materials. // Engng Fract Mech. 71, 2004, pp. 1177-99.
[29] Sedmak, A.; Anyiam, H. A. Structural Integrity Assessment Using Fracture Mechanics. // Structural Integrity and Life, 1, 2(2001), pp. 67-73.
[30] Adžiev, T.; Sedmak, A., Adžiev, G., Arsić, M. Residual Strength Assessment of Cracked Welded Spherical Storage Tank, Structural Integrity and Life, 2, 1-2(2002), pp. 20-22.
[31] Kozak, D.; Gubeljak, N.; Konjatić, P., Sertić, J. Yield load solutions of heterogeneous welded joints. // International journal of pressure vessels and piping, 86, (2009), pp. 807-812.
[32] Dobrojević, M.; Sedmak, A.; Argob, E.; Popović, O. Effects of Geometry and Material Heterogeneity Properties to Behaviour of Charpy Specimen. // Structural Integrity and Life, 3, 2(2003), pp. 73-83.
[33] Adžiev, G.; Sedmak, A. Integrity Assessment of Spherical Storage Tank. // Structural Integrity and Life, 3, 2(2003), pp. 93-98.
[34] Kozak, D.; Vojvodič-Tuma, J.; Gubeljak, N.; Semenski, D. Factors Influencing the Yielding Constraint for Cracked Welded Components. // Materiali in tehnologije, 39, 1-2(2005), pp. 29-36.
[35] Argoub, E. O.; Sedmak, A.; Essamei, M. A. Structural Integrity Assessment of Welded Plate with a Crack. // Structural Integrity and Life, 4, 1(2004), pp. 39-46.
[36] Sedmak, S.; Sedmak, A. Integrity of Penstock of Hydroelectric Power plant. // Structural Integrity and Life, 5, 2(2005), pp. 59-70.
[37] Adžiev, G.; Sedmak, A.; Adžiev, T. Numerical analysis of tensile specimen fracture with crack in HAZ. // Structural Integrity and Life, 8, 2(2008), pp. 107-113.

[38] Manjgo, M.; Sedmak, A.; Grujić, B. Fracture and fatigue behaviour of NIOMOL 490K welded joint. // Structural Integrity and Life, 8, 3(2008), pp. 149-158.
[39] Gubeljak, N.; Predan, J.; Rak, I.; Kozak, D. Integrity assessment of HSLA steel welded joint with mis-matched strength. // Structural Integrity and Life, 9, 3(2009), pp. 157-164.
[40] Kozak, D.; Konjatić, P.; Matejiček, F.; Damjanović, D. Weld Misalignment Influence on the Structural Integrity of Cylindrical Pressure Vessel. // Structural Integrity and Life, 10, 2(2010), pp. 153-159.

Authors' addresses
Adrese autora

Mr. Bashir Younise, PhD student
University of Belgrade
Faculty of Mechanical Engineering
Kraljice Marije 16, 11000 Belgrade, Serbia
E-mail: bsmy2000@yahoo.com

Professor Marko Rakin
University of Belgrade
Faculty of Technology and Metallurgy
Karnegijeva 4, 11000 Belgrade, Serbia
E-mail: marko@tmf.bg.ac.rs

Mr. Bojan Medjo, PhD student
University of Belgrade
Faculty of Technology and Metallurgy
Karnegijeva 4, 11000 Belgrade, Serbia
E-mail: bojanmedjo@gmail.com

Professor Nenad Gubeljak
University of Maribor
Faculty of Mechanical Engineering
Smetanova 17, SI-2000 Maribor, Slovenia
E-mail: nenad.gubeljak@uni-mb.si

Professor Dražan Kozak
J. J. Strossmayer University of Osijek
Mechanical Engineering Faculty in Slavonski Brod,
Trg Ivane Brlić-Mažuranić 2, HR-35000 Slavonski Brod, Croatia
E-mail: dkozak@sfsb.hr

Professor Aleksandar Sedmak
University of Belgrade
Faculty of Mechanical Engineering
Kraljice Marije 16, 11000 Belgrade, Serbia
E-mail: aleksandarsedmak@yahoo.com